Predicting attentional focus: Heartbeat-evoked responses and brain dynamics during interoceptive and exteroceptive processing

Emilia Fló [ID][a,b,*], Laouen Belloli[a,c], Álvaro Cabana[b], Alessia Ruyant-Belabbas [ID][a], Lise Jodaitis[d], Melanie Valente[d], Benjamin Rohaut[a,d], Lionel Naccache [ID][a,d], Mario Rosanova[e], Angela Comanducci[f,g], Thomas Andrillon [ID][a] and Jacobo Sitt[a,*]

[a]Institut du Cerveau—Paris Brain Institute—ICM, Inserm, Sorbonne Université, CNRS, APHP,Hôpital de la Pitié Salpêtrière, 75013 Paris, France
[b]Facultad de Psicología, UdelaR, Instituto de Fundamentos y Métodos, 11200 Montevideo, Uruguay
[c]Consejo Nacional de Investigaciones Científicas y Técnicas (CONICET), Ministry of Science, Technology and Innovation, C1425FQB Buenos Aires, Argentina
[d]Département de Neurophysiologie, Assistance Publique—Hôpitaux de Paris, Groupe Hospitalier Pitié-Salpêtrière, Charles Foix, Sorbonne Université, 75013 Paris, France
[e]Department of Biomedical and Clinical Sciences, University of Milan, 20157 Milan, Italy
[f]IRCSS Fondazione Don Carlo Gnocchi ONLUS, 20162 Milan, Italy
[g]Università Campus Bio-Medico di Roma, 00128 Rome, Italy
*To whom correspondence should be addressed: Emails: emilia.flo.rama@gmail.com, jacobo.sitt@icm-institute.org
Edited By Stephen Fleming

Abstract

Attention shapes our consciousness content and perception by increasing the probability of becoming aware and/or better encoding a selection of the incoming inner or outer sensory world. Engaging interoceptive and exteroceptive attention should elicit distinctive neural responses to visceral and external stimuli and could be useful in detecting covert command-following in unresponsive patients. We designed a task to engage healthy participants' attention toward their heartbeats or auditory stimuli and investigated whether brain dynamics and the heartbeat-evoked potential (HEP) distinguished covert interoceptive–exteroceptive attention. Exteroceptive attention yielded an overall flattening of the power spectral density (PSD), whereas during interoception, there was a decrease in complexity, an increase in frontal connectivity and theta oscillations, and a modulation of the HEP. Subject-level classifiers based on HEP features classified the attentional state of 17/20 participants. Kolmogorov complexity, permutation entropy, and weighted symbolic mutual information showed comparable accuracy in classifying covert attention and exhibited a synergic behavior with the HEP features. PSD features demonstrated exceptional performance (20/20). Command-following was assessed in five brain-injured patients with a modified version of the task. An unresponsive wakefulness syndrome/vegetative state patient and a locked-in syndrome patient demonstrated a willful modulation of the HEP and together with the explored brain markers suggest that patients were complying with task instructions. Our findings underscore the importance of attentional mechanisms in shaping interoceptive and exteroceptive sensory processing and expand the framework of heart–brain interactions employed for diagnostic purposes in patients with disorders of consciousness.

Keywords: interoception, HEP, exteroception, attention, disorders of consciousness

> ### Significance Statement
>
> We show that directing attention to heartbeats or sounds induces distinct brain responses, enabling the identification of covert attention to internal or external stimuli at the individual level. In a small group of brain-injured patients, we tested the potential of our task and the brain markers explored to detect command-following in patients with disorders of conscious. We show evidence of attention-driven changes in the cortical responses to heartbeats and brain dynamics during interoceptive–exteroceptive attention in a patient with unresponsive wakefulness syndrome and in a locked-in syndrome patient, suggesting higher levels of residual consciousness than conveyed behaviorally.

Introduction

The brain continuously monitors the bodily and environmental signals, and the interplay between interoception and exteroception determines whether a change in the system comes from within or from outside, triggering and shaping appropriate allostatic and behavioral responses (1–3). Although visceral signals are typically diffuse and not accessible to our conscious experience, interoception is considered to have a decisive role in

perception, homeostatic responses, and motivational behaviors (4–7). Recent research has demonstrated that bodily rhythms contribute to general brain dynamics influencing cognition at multiple time scales (8–10). Furthermore, certain theories of consciousness propose that the monitoring of visceral information provides the first-person perspective required to define the limits between oneself and the outside, enabling internal and external awareness (4, 11).

Interoceptive attention

Attention has been described as a general mechanism that increases the detection of a desired signal while suppressing the response to irrelevant stimuli (12, 13). The modulatory effect of attention on sensory processing has been consistently shown for top-down attention on sound (14, 15), touch (16), vision (17, 18), olfaction (19), and taste (20). Crucially, visceral information can not only be passively filtered by the brain but attention can also be directed toward bodily signals in a process known as interoceptive attention (5) impacting its cortical representation, which has been evidenced during interoceptive attention to respiratory cycle (21), and to the heartbeats (22).

The heartbeat-evoked potential

The heart has been the preferred candidate to assess the effects of interoceptive attention at the individual level. The heartbeat is triggered by a dynamical pacemaker that is modulated by efferent brain pathways and informs the brain by ascendant pathways (23, 24), of which subjects are normally unaware. Brain response to the heartbeats can be measured by averaging time-locked electroencephalogram (EEG) activity to the electrocardiogram (ECG) waveform R peak (25). The resulting heartbeat-evoked potential (HEP) is considered to reflect the cortical processing of heart activity with and without awareness (26). The amplitude of the HEP is modulated by directing attention to the heart (22, 27, 28), correlates with the accuracy in heartbeat detection (28, 29), and decreases with sleep depth (30).

Brain dynamics during interoceptive and exteroceptive attention

Multiple processes related to top-down attention, such as resource allocation, dynamical focus, inhibition, and selection, have been associated with cortical oscillations and their entrainment (31–35). While brain dynamics of sensory processing have been extensively studied in the context of top-down attention for various exteroceptive modalities, investigations specifically comparing the electrophysiological response during interoceptive attention to the heart and exteroceptive attention remain limited. Two studies based on visual and heartbeat detection tasks reported a trade-off between the HEP amplitude and visually evoked potentials during interoceptive attention, accompanied by an increase in parieto-occipital alpha power (36, 37). In intracranial recordings, increases in high-frequency oscillations (35–110 Hz) in interoception-related cortical regions during heartbeat tapping and an increase in lower frequencies (1–35 Hz) when participants were tapping following an external rhythm have been observed (38). Together, these results suggest that time locked and ongoing brain dynamics during interoceptive and exteroceptive attention can provide information on whether attention is oriented toward the internal or the external world.

Perceptual learning and attention

Casting attention to a specific sensory channel may also enhance the representation of a stimulus that individuals are not actively scanning or may even be unaware of. An interesting case is posited by the perceptual learning of statistical regularities in noise. In the auditory modality, it has been shown that cross-trial repetitions of identical white noise fragments can result in persistent memory formations as indexed by participant's detection accuracy (39, 40), memory-evoked potentials (41), and intertrial phase coherence (ITPC) in the delta band (41, 42). Although the random white noise snippets have no semantic information or salient spectral features, their encoding is long lasting (39), and brain signatures of a mnemonic response are elicited even when the repetitions are unbeknownst to the participants (41, 43). Evidence on the effects of attention on implicit learning of these random acoustic patterns suggests that diverted attention hinders perceptual learning of the repetitions (43). Accordingly, orienting attention toward bodily rhythms should result in a worse encoding of these inconspicuous regularities, reflecting interoceptive or exteroceptive attention despite stimuli being hidden and orthogonal to task demands.

Covert attention in unresponsive patients

As specified above, cortical and cardiac responses to external and internal stimuli are influenced by attention and could therefore be used to detect covert attention. Developing measures of covert attention at the individual level can have major clinical implications as it could be applied to improve the detection of command-following responses (44–46) in noncommunicative patients, such as patients who suffer from disorders of consciousness (DoC) (47). Assessing the level of awareness in these patients poses a significant challenge as expertise is required to differentiate between reflexes and volitional behavior (48) and overt responses may be impaired (49). Indeed, the distinction of unresponsive wakeful syndrome, also referred to as vegetative state (UWS/VS), characterized by arousal without purposeful responses, from the minimally conscious state (MCS), where signs of intentional behavior are occasionally present, leads to significant misdiagnosis rates (50). Moreover, some patients show a dissociation between behavior and brain response, referred to as cognitive motor dissociation (51), where residual consciousness can only be detected by functional neuroimaging methods. Finally, patients with locked-in syndrome (LIS), who are conscious but cannot show responses due to severe paralysis, may initially be misdiagnosed as UWS/VS (52). In this clinical scenario, active paradigms that measure command-following but that do not demand motor or verbal responses are especially appropriate, and a positive result provides significant information on the level of consciousness (53). Crucially, probing the ability to recognize external and internal signals would give essential information on the level of self-awareness of these individuals.

This study

We propose a task based on sustained selective attention to compare the effects of interoceptive and exteroceptive attention on the encoding of heartbeats, and salient auditory targets, as well as their effect on the perceptual learning of inconspicuous repetitions of white noise. We hypothesized that increased attention to the heartbeats should elicit an increased brain response to internal rhythms and a decreased response to the external stimuli, with an opposite pattern during exteroceptive attention. Directing attention to an external sound or to the heartbeats should be
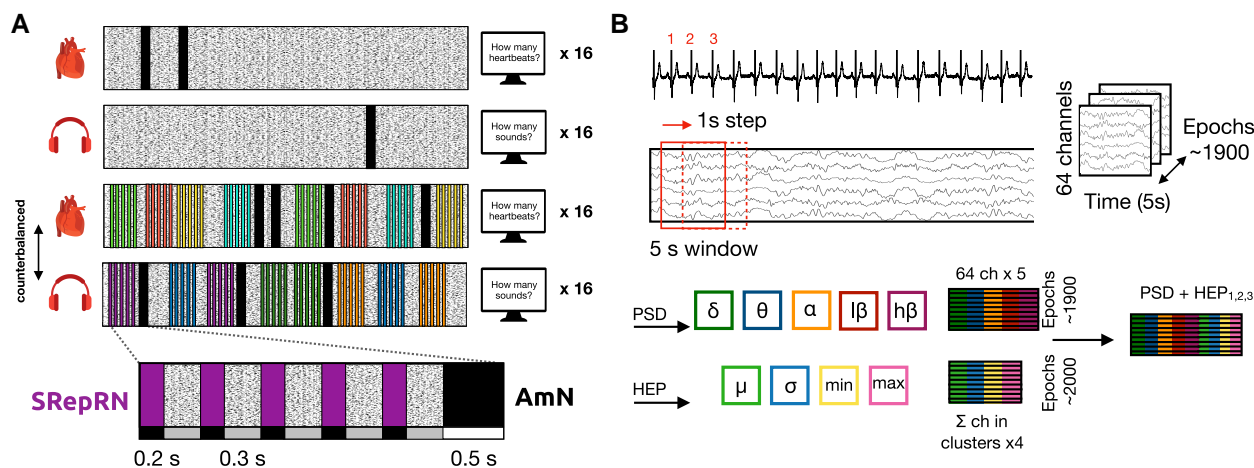
Fig. 1. Experimental design and subject-level analysis. A) The task consisted of 64 trials of 31 s of continuous white noise with bursts of AmN at random times (represented with black lines over noise). On each trial, participants were instructed to focus their attention on the white noise (32 trials) or their heartbeats (32 trials) and were asked to report the counted number (AmN or heartbeats) at the end of each trial. Half of the trials had embedded snippets of repeated white noise within and between trials (SRepRN). Half of the participants were exposed to a set of four RepRN during the sound condition (represented with darker colored lines) and to another set of four RepRN during the heart-attention condition (represented with lighter colored lines), this was counterbalanced across participants, such that each participant was exposed to a specific noise repetition in only one attentional condition. B) For the HEP classifier, for each participant, a cluster permutation analysis was carried out to test for differences in HEP in the remaining participants. The channels and time points in the canonical clusters were used to extract the HEP features on the left-out subject data. For each electrode taking part in the clusters, the mean (μ), the SD (std), the minimum (min), and the maximum (max) voltage in the time window spanning the cluster were extracted for each epoch of the subject withheld from the clustering analysis. For the PSD subject-level classifier, each trial was divided into 5-s sub-epochs using a sliding window with a 1-s step, resulting in a 4-s overlap between epochs. Power was obtained for each sub-epoch and averaged over the delta, theta, alpha, low-beta, and high-beta bands, resulting in five spectral features per channel. As an example of the combined classifiers, the PSD + HEP classifier combining both spectral and time-locked features is represented. The HEP features were derived from the average brain response to the heartbeats occurring within the 5-s sub-epoch, from which the spectral features were also extracted (i.e. heartbeats 1, 2, and 3 for the time window selected).

characterized by specific brain dynamics and should influence the ability to learn regularities passively. Importantly, we elaborated this study with the underlying motivation of applying this paradigm to obtain insights about the nature of attentive processes, and therefore, our main goal was to investigate the suitability of different cortical and bodily measurements as markers to predict attentional focus at the individual level. Finally, we probed the clinical potential of our task on a small cohort of brain-injured patients.

Results

We presented white noise with embedded salient auditory targets only (AmN), or with the same targets together with specific white noise repetitions to which participants were naive (RepRN; Fig. 1A). Exteroceptive attention or interoceptive attention was elicited by asking participants at the beginning of each trial to report the number of targets or the number of heartbeats they felt. EEG, ECG, and respiration were recorded. Event-related potentials, rhythmic and aperiodic EEG activity, complexity, and connectivity were assessed at the group level, and subject-level classifiers were used together with time-locked and dynamical features to classify attentional focus (Table S2). Finally, an adapted version of the task was presented to a small group of unresponsive patients.

Task performance of healthy participants: heartbeats and AmN count

Healthy participants were able to focus their attention on the sound during sound-attention trials, as shown by the proportion of AmN reported (Fig. 2A). The performance during interoceptive attention showed greater variability across participants but a correlation between interoceptive and exteroceptive accuracy was found ($\rho(20) = 0.63$, $P = 0.002$), suggesting an overall engagement in the task. In order to maximize brain responses to the noise repetitions, trials had a high density of RepRN, importantly, the RepRN did not interfere with participants' ability to detect their own heartbeats, as interoceptive accuracy did not differ between trials with plain white noise and trials with embedded noise repetitions (ANOVA $F(1, 21) = 0.056$, $P = 0.82$; Fig. S3). Since detecting AmN was effortless for participants, performances below 70% were seen as a lack of engagement in the task. As a result, we excluded two subjects from further analysis.

Heart activity and respiration are not modulated by exteroceptive–interoceptive attention

Mean heart rate (HR) and mean HR variability (HRV) were measured for each 31-s trial and were contrasted during heart- and sound-attentional conditions (see Supplementary Material). There were no differences in HR (HR heart = 75.13 beats per minute [BPM], HR sound = 75.44 BPM, $t = 0.94$, $P = 0.36$, $\beta = 0.26$, 95% credible interval (CrI) = [−0.43, 0.96], BF = 0.14), nor in HRV (HRV heart = 32.88 ms, HRV sound = 33.15 ms, $t = 0.32$, $P = 0.75$, $\beta = 0.39$, 95% CrI = [−1.38, 2.17], BF = 0.12) between conditions (Fig. 2B). To assess whether the AmN prompted a cardiac deceleration, the interbeat intervals for the first, second, and third heartbeats following sound onset were compared with baseline (see Supplementary Material). Independently of condition, there was no effect of AmN presentation on the interbeat intervals posttarget ($\Delta IBIB0 = 2.13$, $t = 0.85$, $P = 0.39$, $\Delta IBIB1 = 0.67$, $t = 0.27$, $P = 0.79$, $\Delta IBIB2 = -1.88$, $t = -0.75$, $P = 0.45$; Fig. S1B). Moreover, attention did not affect the ECG waveform as suggested by the negative results obtained for a point-by-point analysis (Fig. S1A)
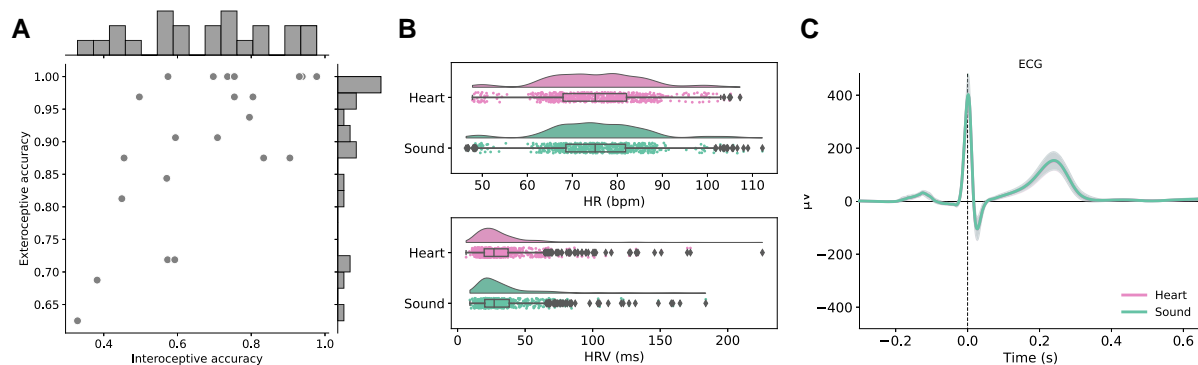
Fig. 2. Task performance across subjects and heart activity. A) Correlation between exteroceptive accuracy as the percentage of AmN reported over the total number of AmN presented during trials of sound-directed attention and the mean interoceptive accuracy across trials of heart-directed attention. B) HR (top) and HRV (down) for all trials during heart and sound-directed attention. C) Average ECG waveform for all subjects during sound and heart-attention conditions with a 95% bootstrap CI.

as well as a by a temporal cluster analysis (minimum cluster $P = 0.46$). Furthermore, we tested whether our task prompted changes in respiratory activity that could influence brain responses to internal and external signals. Respiratory frequency did not differ across conditions (BR heart = 0.249 Hz, BR sound = 0.247 Hz, $t = -0.61$, $P = 0.54$), nor were there differences in the coefficient of variation of the breathing rate (CVBR heart = 0.174, CVBR sound = 0.166, $t = -1.28$, $P = 0.20$; Fig. S3).

HEP and AmN-evoked responses are oppositely modulated by interoceptive and exteroceptive attention

The effect of attention on the cortical response to the heartbeats (HEP) was evaluated with a cluster permutation analysis (see Group-level EEG analysis in Supplementary Material). The analysis revealed two significant clusters. A posterior cluster comprised of 26 channels spanning from 179 to 318 ms (t-sum = 1,382, $P = 0.022$) such that voltage was higher during heart-attention condition, and an anterior cluster comprised of 20 electrodes from 175:316 ms (t-sum = $-1,398$, $P = 0.022$), for which voltage was more negative when attention was directed toward the heart (Fig. 3B). The difference in amplitude for the HEP did not correlate with the subject's interoceptive accuracy, and not all participants showed this modulation (Fig. S4A and B). An increase in ITPC for the delta band was observed in posterior electrodes (t-sum = 7,480, $P < 0.001$, time = -25:600 ms; Fig. S4C), and for ITPC in the theta band (t-sum = $-1,381$, $P = 0.049$, time = 344:600 ms). Moreover, no differences in power were obtained for the frequency bands tested, suggesting that the changes in the HEP are a result of phase modulations at low frequencies. Differences in brain response to amplitude-modulated noise targets (AmN) during the attentional conditions were also assessed using cluster permutation analysis. An increased response to AmN was observed when attention was directed to the sound (Fig. 3A) as indexed by five significant clusters spanning from 68 to 850 ms. We report here two of the clusters that summarize the topography of the effect. A later posterior cluster from 377 to 675 ms (t-sum = $-13,983$, $P < 0.001$) and an early anterior cluster spanning the interval between 68 and 367 ms (t-sum = $-8,184$, $P < 0.002$).

Interoceptive–exteroceptive attention and perceptual learning

In order to assess the effects of interoceptive attention to the heart and attention to sound to inconspicuous noise repetitions, evoked responses to the white noise repetitions (RepRN) and plain white noise (RN) were compared within each condition. Voltage differences were found between the RepRN and RN during sound attention as indexed by a widespread cluster (time = 0–209 ms, t-sum = 5,586, $P = 0.003$). In addition, ITPC coherence in the delta band was higher during sound attention to the concatenations of noise repetitions (structured repetitions, SRepRN) compared with trials with plain white noise (time = 1.40–2.57 s, t-sum = 23,072, $P = 0.009$; Fig. S5C), and no difference in power was found (clusters $P > 0.13$). Conversely, no differences were obtained for the analog analyses between RepRN during trials of heart-directed attention and trials in which attention was directed to the heart but plain white noise was presented (Fig. S5D). In order to assess perceptual learning during heart and sound attention, evoked responses to the first to the fifth RepRN forming the SRepRN stimuli were separately averaged. Nevertheless, no positive results were obtained from the comparison of the first to fifth RepRN against plain white noise within each condition (Fig. S5B).

Rhythmic and aperiodic activity during heart and sound attention

Brain oscillatory and aperiodic dynamics were contrasted between heart and sound-directed attention trials (see Supplementary Material). A group effect of attentional condition was found for the aperiodic activity. Specifically, during interoceptive attention, the aperiodic exponent of the power spectrum was lower than during exteroceptive attention, and this effect was centrally localized in the scalp (t-sum = 24.37, $P = 0.007$). In addition, differences were found in the oscillatory activity. The bandwidth of the beta-band peak was smaller (t-sum = -8.25, $P = 0.014$), and frontal theta power (t-sum = 9.80, $P = 0.028$) was higher during heart-directed attention (Fig. 4A and C).

Complexity and connectivity group analysis

Brain dynamics during attention to the heartbeats and the sound were contrasted using Kolmogorov complexity (KC), permutation entropy (PE), and weighted symbolic mutual information (wSMI). KC was lower during interoceptive attention as shown by a widespread frontocentral parietal cluster (t-sum = -112.77, $P = 0.001$). In addition, connectivity was higher during attention to the heart trials as indexed by an increase in wSMI in a frontal cluster (t-sum = 17.87, $P = 0.026$). Finally, PE was lower during interoceptive attention in centroparietal electrodes (t-sum = -23.39, $P = 0.032$; Fig. 4B).
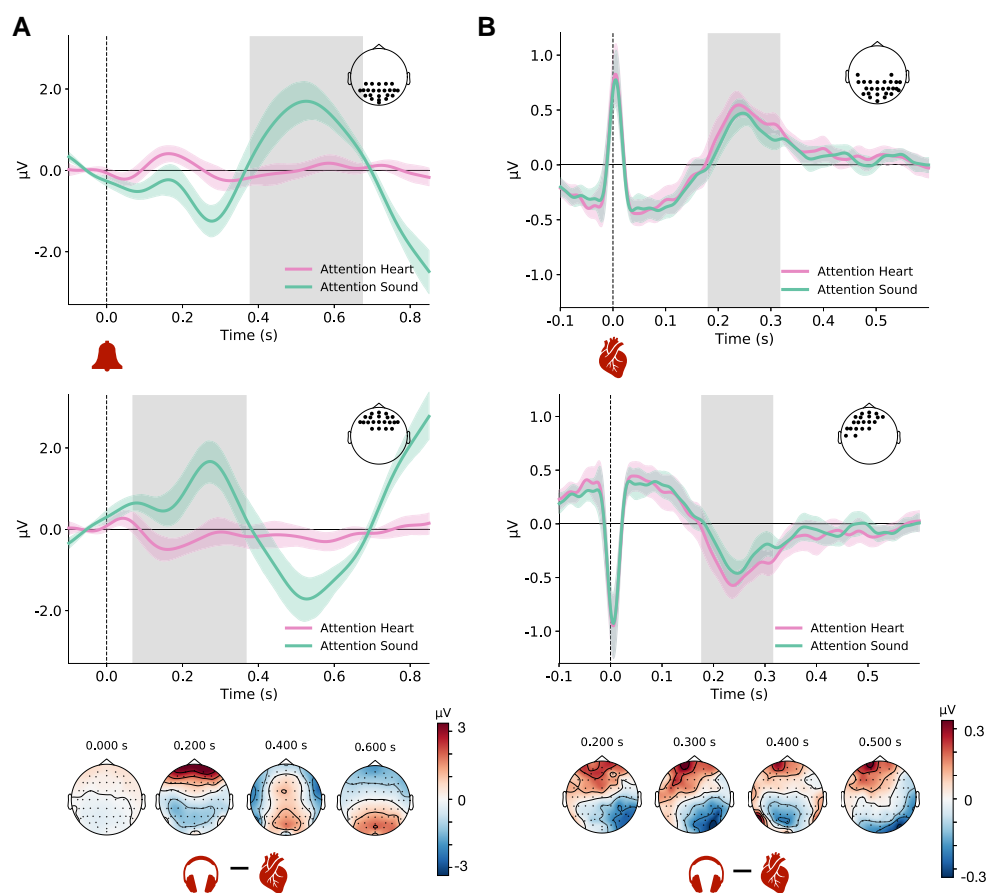
Fig. 3. HEP and AmN evoked are oppositely modulated by interoceptive and exteroceptive attention. A) Brain response to AmN (sound onset at 0 s). An early anterior (68 to 375 ms, *t*-sum = −9,415, *P* < 0.001) and a later posterior (377 to 675 ms; *t*-sum = −13,983, *P* < 0.001) significant clusters were found. B) HEP during heart and sound attention (heartbeat onset at 0 s). Two significant clusters were obtained. A posterior cluster spanning from 179 to 318 ms (*t*-sum = 1,382, *P* = 0.022) and an anterior cluster from 175 to 316 ms (*t*-sum = −1,398, *P* = 0.022). The topography below each plot is the voltage difference between heart and sound conditions. Gray shading marks the temporal span of clusters and black dots indicate channels in clusters. The ERPs shown are the average voltage across channels for each cluster with a 95% bootstrap CI.

Time-locked activity, power, connectivity, and complexity classifiers

Subject-level Adaboost classifiers were implemented using the features for each of the individual markers (HEP, PSD, PE, wSMI and KC) and by combining the time-locked information (mean, standard deviation, minimum and maximum for the cortical response to each heartbeat) with the features of each dynamical marker (PSD, PE, wSMI, KC) (Table S2). Classifiers based on power across the delta, theta, alpha, low, and high beta showed the best performance, accurately classifying all participants' attentional condition with an overall area under the receiver operating characteristic curve (AUC) = 0.75 ± 0.10, with a performance superior to the one obtained for per-band classifiers (Figs. 5A, S6, and S7). The classifier based on the HEP features classified above chance 17 out of 20 participants with a mean AUC = 0.55 ± 0.03, and the AUC score was correlated to the number of epochs ($\rho(18)$ = 0.46, *P* = 0.043) which was not the case for the power spectral density (PSD) classifier ($\rho(18)$ = 0.19, *P* = 0.41), suggesting that increasing the amount of data would yield more accurate results for HEP-based classifiers. The ECG classifier only classified above chance six participants (AUC = 0.50 ± 0.06), which was unsurprising as no differences in cardiac activity were found in the group analyses. These participants showed differences in the ECG in a time window consistent with the group cortical effect. Complexity and connectivity-based classifiers showed comparable performance with the HEP-based classifier. The PE-based classifier was able to classify 17 participants (AUC = 0.59 ± 0.06), the wSMI-based classifier resulted in 16 participants being classified above chance (AUC = 0.57 ± 0.07) and the classifier based on KC accurately classified 18 participants (AUC = 0.59 ± 0.06; Figs. 5A and S7). No significant improvement in classification was obtained for the combination of spectral and HEP features (AUC = 0.75 ± 0.09, *t* = −1.48, df = 19, *P* = 0.92) nor when combined with KC features (AUC = 0.60 ± 0.06, *t* = 1.57, df = 19, *P* = 0.066). Nevertheless, an increase in overall classification was obtained when combining the time-locked features to PE (AUC = 0.61 ± 0.05, *t* = 3.63, df = 19, *P* < 0.001) with three more participants classified (20/20), and to wSMI (AUC = 0.59 ± 0.07, *t* = 3.01, df = 19, *P* < 0.001), with two more participants classified (18/20; Fig. 5B).

Brain-injured patients show a modulation of the HEP and ongoing brain activity consistent with command-following

Three UWS/VS, one MCS−, and a LIS-diagnosed patients were presented with a modified version of the task (see Supplementary Material). Feature extraction was carried out and fed to classifiers to differentiate between trials of heart- or sound-directed attention as a proxy measure for command-following. For the LIS
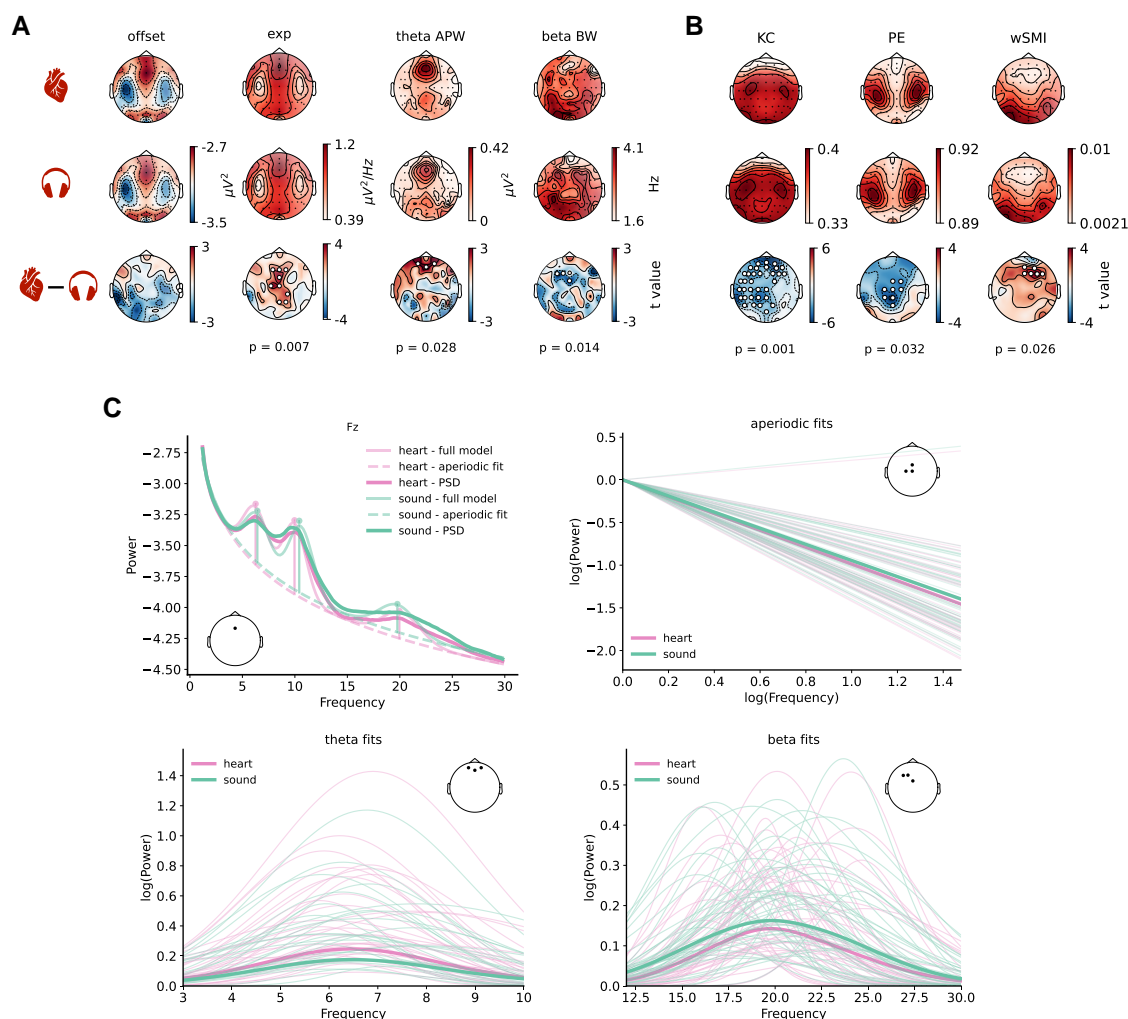
Fig. 4. Interoceptive and exteroceptive attention show different brain dynamics. A) Periodic and aperiodic components of the power spectrum model fit during heart-attention trials (top), sound-attention trials (middle), and *t*-values for the difference between the components during both conditions (bottom). From left to right: offset value (off), aperiodic exponent (exp), and aperiodic-adjusted power (APW), and bandwidth (BW) for theta and beta bands. B) KC, PE, and wSMI. Top: markers topography during attention to the heart. Middle: markers topography during sound attention. Bottom: *t*-values for the difference between markers during heart- and sound-attention trials. White dots indicate sensors in significant clusters. C) Left top: average PSD for channel Fz with aperiodic and periodic model components for each condition. Right top: aperiodic fits for all subjects and conditions for Cz, C1, and FCz (a subset of channels were selected for visualization purposes). Bottom left: periodic fits for the theta range (4:8 Hz) for all subjects and conditions for channels Fp1, Fp2, and AFz. Bottom right: periodic fits for the beta range (15:25 Hz) for all subjects and conditions for channels F3, FC1, and FCz.

patient, we expected a brain response consistent with the one elicited during the interoceptive and exteroceptive attention conditions in healthy participants as these patients are conscious. Although UWS/VS are patients who clinically do not show responses to the external world and MCS− are individuals who show basic cortically mediated behaviors, such as visual fixation and pursuit and automatic responses (54, 55), in a misdiagnose scenario covert volitional responses could be present.

P1 (UWS/VS) was only classified by KC (AUC = 0.56 ± 0.03, $P = 0.014$, all rest $P > 0.09$). P2, also a UWS/VS patient, was classified above chance by the PSD features (AUC = 0.56 ± 0.03, $P = 0.029$), and although the HEP features were not sufficient for an above chance classification (AUC = 0.51 ± 0.01, $P = 0.38$), combining these time-locked features with the spectral and KC information improved the AUC scores (PSD: AUC = 0.58 ± 0.03, $P = 0.002$; KC: AUC = 0.60 ± 0.03, $P = 0.002$) yielding a successful classification. No EEG marker could differentiate between attentional conditions for UWS/VS patient P3. The attentional state of patient in LIS (P4) was not

classified by the single marker classifiers, but combining the HEP features with the PSD, KC, and PE resulted in an above-chance classification (PSD + HEP: AUC = 0.54 ± 0.02, $P = 0.042$; KC + HEP: AUC = 0.55 ± 0.02, $P = 0.013$; PE + HEP: AUC = 0.55 ± 0.02, $P = 0.026$). Finally, the MCS− patient tested at the Milan center (M1) was successfully classified only by the PE features (PE: AUC = 0.56 ± 0.02, $P = 0.007$; Fig. 6A). Both patients who showed increased AUC scores when incorporating the HEP features (P2 and P4) show a modulation of this ERP on a time window and electrodes consistent with healthy participants' responses (Fig. 6B). A modulation of the HEP was not observed for the rest of the patients.

Discussion

The present study aimed to develop and test an experimental paradigm that would allow us to infer the attentional focus of an individual from brain and bodily responses to internal and external stimuli. The hypothesis underlying this work is that
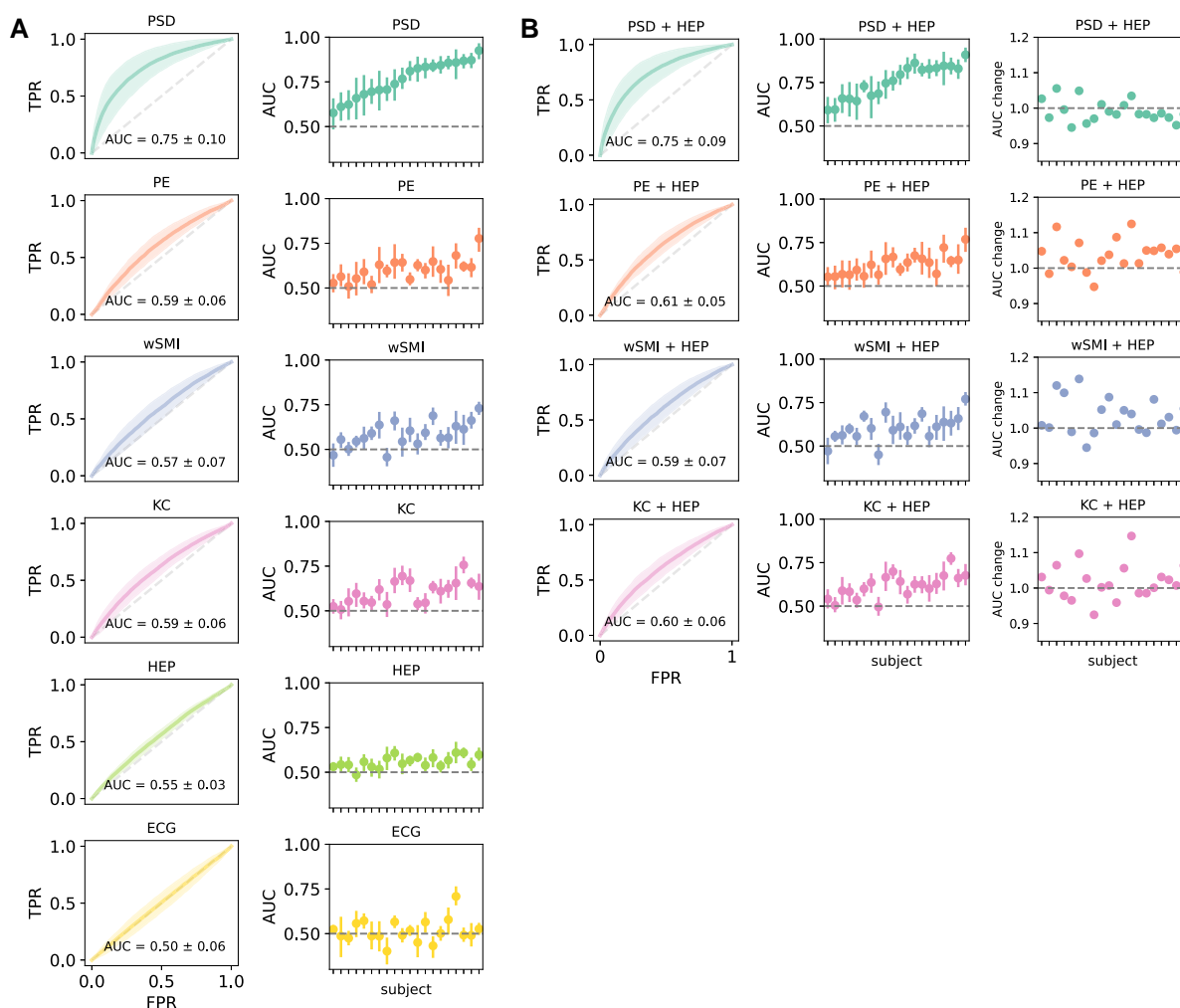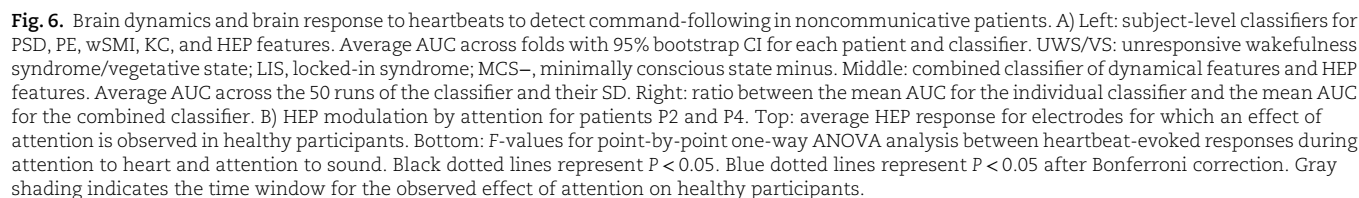
Fig. 5. Brain dynamics and brain response to the heart are informative of attention orientation at the individual level. A). Subject-level classifiers for PSD, PE, wSMI, KC, HEP, and cardiac activity (ECG) features. Left: average receiver operating characteristic (ROC) curves across cross-validation folds and subjects. Shading corresponds to the SD. Right: average AUC across folds with 95% bootstrap CI for each subject and classifier. Subjects are sorted considering the AUC for the spectral density classifier. B) Combined classifier of dynamical features and HEP features. Left: average ROC curves across cross-validation folds and subjects. Shading corresponds to the SD. Middle: average AUC across folds with 95% bootstrap CI for each subject and classifier. Right: ratio between the mean AUC for the individual classifier and the mean AUC for the combined classifier. Subjects are sorted considering the AUC for the spectral density classifier (not combined with HEP features).

attention has an impact on our consciousness content and perception, such that it enhances the probability of becoming aware and, or, of better encoding a selection of the incoming inner or outer sensory world. For this purpose, we designed a task to engage interoceptive and exteroceptive attention by orienting participants to their heartbeats or to salient auditory stimuli, and measured their cortical, cardiac, and respiratory activity, while the effects of attention on passive encoding were probed using concealed noise repetitions.

Interoceptive attention to heartbeats modulates their cortical encoding

In agreement with previous findings (22, 38), our results show that directing attention to the heartbeat yields a modulation of the cortical response to the heartbeats. In addition to replicating the group effect on the HEP during interoceptive attention, we have shown the strong nature of this modulation, showing it can reliably classify attentional states at the single-subject level.

Although HEP amplitude can be modulated by the respiratory cycle (56), exhalation and inhalation showed no differences between attentional conditions. Moreover, no modulation of the cardiac rhythm or the ECG waveform was found at the group level. In addition, cardiac activity was not effective in detecting covert attention. Together, our results suggest that the cortical differences were not driven by changes in the afferent signals but are a result of a top-down modulation on the cortical processing of the heartbeats consistent with predictive coding accounts (57–59). Under this view, visceral sensory representations are shaped by empirical a priori of what the "interocept" should be in terms of content and precision, and how far were they from the afferent inputs, expressed as feedforward prediction error signals. It has been postulated that the computational operation of attention is to optimize the precision of sensory signals by modulating the gain of the prediction feedforward error at particular levels in the hierarchy which would result in increased neural responses to specific features or stimuli in relevant cortical areas (60).

Fig. 6. Brain dynamics and brain response to heartbeats to detect command-following in noncommunicative patients. A) Left: subject-level classifiers for PSD, PE, wSMI, KC, and HEP features. Average AUC across folds with 95% bootstrap CI for each patient and classifier. UWS/VS: unresponsive wakefulness syndrome/vegetative state; LIS, locked-in syndrome; MCS−, minimally conscious state minus. Middle: combined classifier of dynamical features and HEP features. Average AUC across the 50 runs of the classifier and their SD. Right: ratio between the mean AUC for the individual classifier and the mean AUC for the combined classifier. B) HEP modulation by attention for patients P2 and P4. Top: average HEP response for electrodes for which an effect of attention is observed in healthy participants. Bottom: F-values for point-by-point one-way ANOVA analysis between heartbeat-evoked responses during attention to heart and attention to sound. Black dotted lines represent $P < 0.05$. Blue dotted lines represent $P < 0.05$ after Bonferroni correction. Gray shading indicates the time window for the observed effect of attention on healthy participants.

The HEP voltage modulation was accompanied by an increase in ITPC in the delta and theta band, with no differences in power, hinting at a phase-locking reset effect of attention on ongoing neural dynamics. It has been reported that increases in HEP amplitude are associated with increases in ITPC in these frequency bands (30, 61) and that during resting state the heartbeat produces a cortical synchronization in the theta band (62). In this line, we found an increase in theta connectivity in frontocentral electrodes during interoceptive attention as measured by wSMI.

The modulation of the HEP appears to be unaffected by whether participants could detect their heartbeats, as the attention-driven changes in the HEP were not correlated to interoceptive accuracy scores. It is possible that awareness of one's heartbeat is not necessary to trigger cortical changes in heartbeat processing, similar to how hidden noise repetitions were better encoded during sound-attention trials despite going unnoticed by participants. In addition, multiple criticisms concerning the reliability of heartbeat counting have been put forward. Responses can be influenced by the knowledge participants have of their own HRs, and as these tasks are typically measured during rest, the HRV is very small and therefore hard to perceive and report (63). Moreover, it has been reported that the belief about one's own HR is a better predictor of the number counted than the actual quantity of heartbeats (64). Whether the modulation of the HEP is specific to interoceptive processing of the heartbeats (26), an enhancement to somatosensory afferent information from the skin (65), or a general increase in the encoding of visceral signals, cannot be determined by our study. Nevertheless, recent research shows that counting heartbeats and counting respiratory cycles both elicited an increase in the HEP amplitude during an early time window (230 ms) for heartbeats elicited during the exhalation phase, with a modulation for later time windows (400 ms) only during cardiac interoception (66). This suggests that increases in the cortical response to heartbeats are not specific to heartbeat attention, but can occur whenever attention is directed toward visceral signals and interferences by external stimuli are kept low. Regardless of whether the participant's mental content corresponded with a bodily sensation of their heartbeats or some form of general implicit visceral perception, we show that the HEP constitutes an effective marker of internal and external attention.

Exteroceptive attention to sound induces an overall gain in auditory processing

Brain response to AmN was substantially affected by attention. This was expected as participants had to detect an infrequent and salient sound, which typically elicits a P300 response (67). Although the effect of attention on perceptual learning of noise repetitions was not as prominent, the white noise repetitions were better encoded during sound-attention trials, as shown by the ERP and ITPC results. No cortical response was found for the first repetition of the SRepRN, which would have indexed the long-term learning of the snippets and not a within SRepRN short-term learning effect. Our outcome could be the result of a lack of power, and increasing the number of repetitions in future work would clarify this. In fact, although an increased response is visually noticeable for the third repetition during sound attention and the fourth repetition during heart attention in comparison with plain white noise (Fig. S5B), no statistical differences were obtained, supporting the hypothesis that we lacked power. From our results, we can only infer that during exteroceptive attention, there was a discernible enhancement of auditory processing, leading to an overall increase in the brain response to the RepRN. Unlike previous research, our experimental design holds a distinctive advantage. Modulating attentional focus within the same task with all RepRN presented in both conditions across participants makes it less likely that results are driven by some noise seeds being more easily perceived than others and enables measuring concurrent learning effects.

Brain dynamics during heartbeat and sound attention

Multiple studies have focused on comparing the effects of internal attention (68) on the processing of external stimuli using paradigms based on mental operations such as mind wandering (69–73) or mental imagery (73), showing a decrease of sensory evoked potentials during attention to internal information, consistent with our findings. Concerning brain dynamics, these paradigms show increases in alpha power (74, 75) associated with a top-down inhibition of cortical areas that would process distractor-relevant information (76), modulations of theta power reflecting working memory demands (77, 78), and increases in the theta–beta ratio during internal thought production and low alertness (79, 80). However, scarce studies have directly compared brain dynamics during interoceptive and exteroceptive attention. In our study, and following previous research (38), power was lower during interoceptive attention compared with exteroceptive attention for frequencies between 1 and 30 Hz. Our methodological approach allowed us to attribute this difference to an overall change in aperiodic activity such that power at lower frequencies is increased in relation to power at higher frequencies during the interoceptive task. An overall steepening of PSD has been shown during anesthesia (54, 81, 82) as well as during sleep (54), and has mechanistically been attributed to changes in the excitation–inhibition ratio in the brain (55, 82). Functionally, increases in PSD slope have been observed during response inhibition (83, 84), and interpreted as a marker of top-down control required to sustain goal representations (85). During both interoceptive and exteroceptive attention conditions, participants were demanded to carry out a detection operation. Nevertheless, the heartbeats and the auditory stimuli we employed have intrinsically different properties and probably elicited different behaviors. Cardiac activity is a rhythmic stimulus; therefore, counting heartbeats was a repetitive and sustained operation. On the contrary, AmNs occurred randomly and scarcely, and participants would incur in counting none or a few times on each trial. Finally, given the lack of salience of heartbeats, interoceptive-attention trials were probably more demanding for participants, which could explain the observed aperiodic activity differences. In addition, our results show that interoceptive attention was characterized by less complex or regular brain dynamics, with a topographical widespread pattern. Brain signal complexity is associated with the number of independent functional sources, such that the higher the complexity the less correlated the neural sources sustaining the overall activity (86). Lower complexity during interoceptive attention is consistent with a more overall stable brain configuration compared with the exteroceptive attention condition.

Together with changes in the background activity, the beta-band peak was narrower, and theta power was higher during heart-attention trials. As mentioned, previous research has associated a higher theta–beta power ratio with episodes of mind wandering (87) which are typically elicited during sustained and repetitive tasks. Considering that the HEP was modulated during the interoceptive condition, we argue that participants were actively engaged during the task making stimulus-independent thought unlikely, and the rhythmic changes observed would be a reflection of cognitive effort. In line with this, frontal theta has been associated with target detection (88), fatigue (89), and overall cognitive control (90).

PE and wSMI features combined with the HEP information enhanced the classification, signaling that these linear and nonlinear measures convey mutual information. This behavior was

not observed in the case of spectral features or KC. For KC, there was an improvement but it did not reach significance. Possibly, the increase in information could not compensate for the detrimental effect of having a larger number of features in the resulting classifier. The spectral and the HEP classifiers performance were correlated (Fig. S8), which suggest that the time-locked information is already embedded within the signal power decomposition, rendering both groups of features redundant and leading to no improvement. Including all spectral bands as features yielded a better classifier than using each power band by itself, which is consistent with a general change in brain dynamics during our interoceptive–exteroceptive attention manipulation. Overall, the information conveyed by the HEP seems to be particularly relevant to complement nonlinear markers, especially when AUC scores are low and there is potential to improve classification.

HEP and dynamical features act synergically to classify the attentional state of two brain-injured patients

The potential of this tool to detect command-following was probed in a small group of brain-injured patients. Classification by the proposed features showed very different behaviors across patients which is expected in a small sample with such heterogeneous etiologies. P1 showed inconsistent results across classifiers, with PE and PSD classifiers showing a below-chance performance, and KC an above-chance performance. This can occur when the models fit to noise in the training sets and is suggestive of no difference in neural activity during both attentional conditions. P3, behaviorally diagnosed as UWS/VS, did not show AUC values above chance for any of the markers, and M1, a MCS– patient, was only classified by the PE features, likely indexing no command-following behavior. Crucially, the brain responses of the LIS patient (P4) and a patient with a UWS/VS diagnosis (P2) were reliably classified by combining dynamical and HEP features. Although the classification accuracies were lower in these two patients, probably due to less sustained attention and a more noisy environment, the consistency across classifiers together with changes in the cortical responses to heartbeats topographically and temporally consistent with healthy participants' responses suggests that patients were complying with task instructions. The detection of command-following in the LIS represents a positive control of our task as consciousness is preserved in these patients and command-following is therefore expected. Importantly, our assessment suggests that P4 had higher levels of residual consciousness than conveyed behaviorally, and this would mean a mismatch between the patient's conscious level and the clinical diagnosis. Our results expand the framework of heart–brain interactions employed for DoC diagnostic purposes (91–93), by showing for the first-time attention-driven changes in the HEP in two brain-injured patients with severe impairments of sensory, motor, and executive functions. Compared with other command-following tasks (44, 46), our paradigm possesses the advantage of contrasting brain responses to two active instructions (instead of active instructions vs. resting state), which in addition are less demanding compared with executing complex imaginary behaviors or actual movements. Beyond command-following, we argue that the ability to distinguish between internal and external signals in DoC patients could be interpreted as a signature of preserved self-awareness. Moreover, the proposed task can provide information on different levels of information processing independently of the patient following the instructions, as passive

cortical responses to sounds, and heartbeats can be measured, as well as assessing EEG markers that have already proven robust in indexing the state of consciousness in DoC patients (93, 94). Our results are a proof of concept of the potential of this novel tool to detect command-following among patients who are unable to convey explicit behavioral responses and the feasibility of its application in clinical settings. Future work assessing a bigger cohort of patients should be carried out to comprehensively evaluate its diagnostic as well as prognostic capabilities.

Conclusions and future directions

In this work, we explored the modulatory effects of interoceptive–exteroceptive attention on the cortical processing of bodily and auditory signals. We report an overall gain in auditory processing during sound attended trials, as indexed by an increased cortical response to target sounds as well as a better encoding of noise repetitions, and a heightened cortical response for heartbeats when attention was directed to the cardiac rhythm. During the exteroceptive attention condition, an overall power increase across the frequency range of 1–30 Hz was observed, whereas during the interoceptive attention condition, there was a decrease in complexity, together with an increase in theta and a decrease in beta oscillations. Our findings demonstrate that directing attention to the cardiac rhythm and to auditory stimuli elicits distinct neural responses that can be employed to track covert attention at the individual level. Importantly, we show that the brain markers studied in this work can be useful in detecting EEG proxy of command-following in unresponsive patients. Crucially, the proposed paradigm provides multiple layers to explore information processing and awareness in these patients and requires equipment commonly available in clinical environments, rendering its application across centers straightforward.

Materials and methods
Healthy participants

Twenty-two healthy volunteers participated in the task (13 females, average age, 30.63 ± 3.39). All participants reported having normal hearing and had not been exposed to the stimuli before the experiment. The study was approved by the ethics committee of the Facultad de Psicología, Universidad de la República (Uruguay). All participants gave informed consent and were not awarded any economic or academic retribution, according to the nationally established guidelines (Decree N379/008).

Experimental design

The task consisted of 64 trials of 31 s of continuous white noise with bursts of AmN at random times. At the beginning of each trial, participants were instructed binaurally to close their eyes and focus their attention on the white noise (32 trials) or their heartbeats (32 trials), and to count the number of AmN or heartbeats, respectively. At the end of each trial, participants were audiovisually instructed to open their eyes and report the number using the keypad. Participants were not given any specific instruction on how to count their heartbeats but were exhorted to not measure their pulse. Half of the trials had embedded snippets of repeated white noise within and between trials (RepRN) that were not disclosed to participants (Fig. 1A). At the beginning of the experiment, an eight-trial practice took place to ensure that participants understood the task. The practice stimuli were not repeated during the task and the noise repetitions

were different from the ones used in the experiment. Stimuli presentation was coded in Psychopy 3.2.0 (95), and audio files were played using the sound library PTB in Windows 7 together with the Focusrite Scarlett 4i4 USB audio interface. Stimuli were presented binaurally through Etymotic ER3C tubal insert earphones, and sound amplitude was adjusted for each participant during practice trials. The trials were presented in a randomized fashion and the intertrial interval was randomly varied between 5 and 10 s.

Stimuli construction

AmN was constructed by multiplying 0.5 s of the running white noise background with a 40 Hz sinusoid at a modulation depth of 30%. For each trial, between 0 and 4 AmN were randomly included. Half of the trials (32 trials) included a concatenation of five copies of a structured noise repetition composed of a 0.2-s-long white noise snippet (RepRN) seamlessly concatenated to 0.3-s-long fresh noises. Eight different RepRNs were created using different random seeds, such that four appeared during trials in which participants had to focus their attention on the sound (RepRN-Sound) and the other four RepRN were only included in trials of heart-directed attention (RepRN-Heart). The RepRNs assigned to each attentional condition were counterbalanced across participants. In each trial, the four RepRN concatenations were repeated twice, resulting in eight RepRN SRepRN within each trial (Fig. 1A).

Physiological recordings and preprocessing

EEG and ECG signals were recorded using a Biosemi Active-Two system. Sixty-four Ag-AgCl scalp electrodes were placed on a head cap following the location and label of the 10–20 system, flat-type channels were placed on the left and right mastoid bones, and on the left and right collarbones to record cardiac activity. The signals were referenced online to the common mode sense (active electrode) and grounded to a passive electrode (Driven Right Leg). Data were digitized with a sample rate of 512 Hz with a fifth-order low-pass sinc filter with a −3 dB cutoff at 410 Hz. As a backup, a second ECG recording was obtained following the same configuration but with a ground electrode positioned below the neck on the back of participants, and a respiration belt was used to record breathing. Both signals were recorded with a PowerLab 4/30 (ADInstruments) at a 400-Hz sample rate. For two participants, the backup ECG recording was used for the analyses. The analyses were conducted using MNE 1.0.3 (96).

EEG preprocessing

EEG data were processed according to the stimuli and the level of granularity of the analysis of interest, this resulted in seven types of epochs: (i) For the HEP, the data were filtered with a 30-Hz low-pass filter (one-pass zero-phase FIR filter with length 227 samples), epoched −0.5:0.8 s time-locked to the R peak of the ECG waveform, linearly detrended and referenced to the average of all channels. Epochs were not baseline corrected to avoid any contamination from the PQ component of the heartbeat. Heartbeats matching the moment of the AmN presentation were not included. (ii) For the AmN, to remove alpha oscillations due to participants having their eyes closed, data were filtered with bandpass filter 0.2–7 Hz (one-pass zero-phase FIR filter with length 8,449 samples), referenced to the average of all channels, epoched −0.1:0.85 s relative to sound onset, linearly detrended and baseline corrected 100 ms before sound onset. For the white noise repetitions, the data were filtered following the

preprocessing for the AmN but referenced to the average of the two mastoid electrodes. Subsequently, data underwent two types of epoching: (iii) −0.4:3 s relative to sound onset thus comprising the five noise repetitions (SRepRN), and (iv) from −0.05:0.5 s relative to each repeated noise (RepRN). For the ERP analysis of the SRepRN and for each RepRN, 0.2 and 0.05 s to sound onset were, respectively, used as a baseline. (v) In order to have a standard against which to compare the activity evoked by the noise repetitions, analog epochs to (iii) and (iv) were obtained from trials with plain white noise. This was carried out avoiding EEG data matching AmN presentation. (vi) For the subject-level analyses, raw data were filtered with a bandpass filter 0.1–30 Hz (one-pass zero-phase FIR filter with length 16,897 samples), and referenced to the average of all channels. The interval between 1:30 s of each 31 s trial (to avoid onset/offset sound artifacts) was segmented into 5 s epochs with an overlap of 4 s. This procedure resulted in a comparable number of trials for the classifiers using ongoing brain activity as features, and HEP-based classifiers, as well as the combination of different families of features (see below). Finally, the 30 s epochs were segmented into (vii) 5 s sub-epochs without overlap for group-level analyses of complexity, connectivity, and power. For all epoch types, autoreject 0.3.1 (97) was used to reject bad epochs and interpolate noisy channels. For all the analyses and participants, the number of observations was equalized between conditions taking into consideration temporal proximity and thus avoiding data imbalance. The ECG artifact (98) could not be completely removed using independent component analysis. Therefore, we decided to keep the potential ECG contributions in the EEG but carry out analyses to check for potential differences in cardiac activity that could be driving our results. We tested for changes in HR and HRV as well as differences in the ECG waveform across conditions.

Subject-level EEG analysis

In order to classify the attentional focus for each participant evoked, connectivity, information theory, and spectral markers were extracted and fed to subject-level classifiers. The evoked features were computed from each brain response to the heart, and the rest of the features were extracted from the 5 s sub-epochs (see Table S2 for the number of features and observations). We followed a similar approach as in Claassen et al. (44), which focuses on developing classifiers that maximize the differences within a subject's data while using appropriate cross-validation and statistical procedures. Adaboost classifiers with decision trees as base estimators (99) were implemented using Scikit-learn v1.0.2 (100). The number of decision trees was set to 1,000, and the maximum depth of each decision tree was set to 1. The splitting criteria used for each decision tree was set to "gini." We followed a grouped stratified k-fold cross-validation procedure with 8-folds where on each fold all sub-epochs (or brain response to the heart) from the same trial were grouped either in the train or test data to avoid data leakage, such as correctly identifying sub-epochs due to finding similarities in sub-epochs of the same 31 s trial. Importantly, all parameters were the same across participants and were defined before collecting patient data. We worked with a balanced dataset such that for every classifier half of the observations corresponded to sound-attention trials and half corresponded with heart-attention trials. For each classifier, the mean accuracy across folds, measured as the AUC, was obtained and significance was evaluated using a nonparametric statistical approach (101). The labels for the observations were randomly permuted 500 times and for each permutation, the mean classifier accuracy

was obtained. We compared the mean accuracy of our original data against the empirical null distribution of classification accuracies. The proportion of null classification accuracies greater than the AUC of the original data yielded our P-values. The level of significance was established at $a = 0.05$. The resulting P-values were corrected using the false discovery rate method ([102]).

HEP features

In order to obtain the HEP features a leave-one-out approach was implemented as follows. Cluster permutation analyses were carried out on all subjects except the subject for which the feature extraction and subsequent classification were going to be computed. For the canonical clusters obtained, clusters with $P < 0.05$ were selected. For each electrode taking part in the selected clusters, the mean, the SD, and the maximum and the minimum voltage in the time window spanning the cluster were extracted for each epoch of the subject withheld from the clustering analysis. This resulted in four features per channel in the clusters. As a control, the same temporal windows were used to extract analog features from the ECG channel resulting in four features per cluster.

Spectral, complexity, and connectivity features

For each subject, a Laplacian transformation ([103]) was applied on the channels of the 5 s sub-epochs to reduce the effect of volume conduction and obtain less correlated sensor signals. PSD for frequencies between 1:30 Hz was obtained using multitapers as implemented in the psd_multitaper function in MNE. Power was averaged across delta (1:4 Hz), theta (4:8 Hz), alpha (8:14 Hz), low-beta (14:20 Hz), and high-beta (20:30 Hz) bands for each channel, resulting in 320 spectral features per sub-epoch (5 power features for each of the 64 electrodes). To assess brain dynamics during the interoceptive and exteroceptive attention conditions, PE, wSMI, and KC markers were computed. The selection of these complexity and connectivity markers was driven by previous work showing their efficacy in classifying conscious states in DoC patients ([94], [104]). Furthermore, these metrics capture nonlinear dynamics and complement spectral and time-locked features (see Supplementary Material).

Time-locked and dynamical features

In order to evaluate a synergistic effect of the time-locked and dynamical features to classify attentional focus, combined classifiers were implemented joining the HEP features with each of the dynamical features (power, KC, PE, and wSMI). Brain responses to heartbeats arising during the 5 s sub-epochs were averaged, and from the evoked activity, the HEP features (mean, SD, minimum, and maximum) were extracted, as detailed above (Fig. 1B). If for a sub-epoch, all concurrent heartbeats were discarded during epoch rejection, the median across all the observations was used to replace missing data.

Brain-injured patients

Seven brain-injured patients participated in this study: three patients were assessed at the IRCCS Santa Maria Nascente Fondazione Don Carlo Gnocchi ONLUS, Milan (Italy), and four patients at the Pitié-Salpêtrière Hospital, Paris (France) in the context of the EU-funded multicentric project Perbrain ([105]). Two Milan patients could not complete the task due to technical issues and were discarded from the analysis. The demographics and clinical information for the remaining five patients are listed in Table S1. All patients were in a subacute state (0.5:1.5 months since injury), except for M1 (~8 months since injury), a chronic DoC patient. The assessment was performed following the ethical standards of the Declaration of Helsinki (1964) and its later amendments and was approved by the local committees of each center (Comité de protection des personnes Ile de France I, #2013-A00106-39 and ethics committee section "IRCCS Fondazione Don Carlo Gnocchi" of ethics committee IRCCS Regione Lombardia, protocol number 32/2021/CE_FdG/FC/SA). Informed consent was obtained from the legal guardians of the patients before enrolling them in the study. The Coma Recovery Scale-Revised ([106]) was performed by experienced neurologists on the same day as the task. All patients had behavioral responses to sound or cortical auditory responses assessed with the local-global paradigm ([82], [107]).

Acknowledgments

Supplementary Material

Supplementary material is available at *PNAS Nexus* online.

Funding

Author Contributions

E.F. conceptualization, methodology, formal analysis, investigation, writing—original draft, visualization. L.B. methodology, writing—review & editing, Á.C. methodology, writing—review & editing, A.R-B. investigation (patients), writing—review & editing, L.J. investigation (patients) M.V. investigation (patients), B.R. resources, L.N. resources, writing—review & editing, M.R., resources, writing—review & editing, Á.C. resources, investigation (patients), writing—review & editing, T.A. conceptualization, writing—review & editing, J.S. conceptualization, supervision, writing—review & editing, funding acquisition. All authors have read and approved the manuscript.

Preprints

This manuscript was posted on a preprint: https://doi.org/10.1101/2023.11.03.565584.

Data Availability

The data files and the analysis code used for this study are available on OSF at https://osf.io/r7uqp/.

References

1. Ceunen E, Vlaeyen JWS, Van Diest I. 2016. On the origin of interoception. *Front Psychol.* 7:743.
2. Critchley HD, Harrison NA. 2013. Visceral influences on brain and behavior. *Neuron.* 77:624–638.
3. Petzschner FH, Garfinkel SN, Paulus MP, Koch C, Khalsa SS. 2021. Computational models of interoception and body regulation. *Trends Neurosci.* 44:63–76.
4. Craig AD. 2002. How do you feel? Interoception: the sense of the physiological condition of the body. *Nat Rev Neurosci.* 3:655–666.

5   Joshi V, Graziani P, Del-Monte J. 2021. The role of interoceptive attention and appraisal in interoceptive regulation. *Front Psychol*. 12:714641.

6   Khalsa SS, *et al.* 2018. Interoception and mental health: a roadmap. *Biol Psychiatry Cogn Neurosci Neuroimaging*. 3:501–513.

7   Quadt L, Critchley HD, Garfinkel SN. 2018. The neurobiology of interoception in health and disease. *Ann N Y Acad Sci*. 1428:112–128.

8   Azzalini D, Rebollo I, Tallon-Baudry C. 2019. Visceral signals shape brain dynamics and cognition. *Trends Cogn Sci*. 23:488–509.

9   Draguhn A, Sauer JF. 2023. Body and mind: how somatic feedback signals shape brain activity and cognition. *Pflugers Arch*. 475:1–4.

10 Engelen T, Solcà M, Tallon-Baudry C. 2023. Interoceptive rhythms in the brain. *Nat Neurosci*. 26:1670–1684.

11 Park HD, Tallon-Baudry C. 2014. The neural subjective frame: from bodily signals to perceptual consciousness. *Philos Trans R Soc B Biol Sci*. 369:20130208.

12 Harris KD, Thiele A. 2011. Cortical state and attention. *Nat Rev Neurosci*. 12:509–523.

13 Sarter M, Givens B, Bruno JP. 2001. The cognitive neuroscience of sustained attention: where top-down meets bottom-up. *Brain Res Rev*. 35:146–160.

14 Hall DA, *et al.* 2000. Modulation and task effects in auditory processing measured using fMRI. *Hum Brain Mapp*. 10:107–119.

15 Hillyard SA, Hink RF, Schwent VL, Picton TW. 1973. Electrical signs of selective attention in the human brain. *Science*. 182:177–180.

16 Johansen-Berg H, Christensen V, Woolrich M, Matthews PM. 2000. Attention to touch modulates activity in both primary and secondary somatosensory areas. *NeuroReport*. 11:1237–1241.

17 Corbetta M, Miezin F, Dobmeyer S, Shulman G, Petersen S. 1991. Selective and divided attention during visual discriminations of shape, color, and speed: functional anatomy by positron emission tomography. *J Neurosci*. 11:2383–2402.

18 Kanwisher N, Wojciulik E. 2000. Visual attention: insights from brain imaging. *Nat Rev Neurosci*. 1:91–100.

19 Singh AK, Touhara K, Okamoto M. 2019. Electrophysiological correlates of top-down attentional modulation in olfaction. *Sci Rep*. 9:4953.

20 Luo Q, Ge T, Grabenhorst F, Feng J, Rolls ET. 2013. Attention-dependent modulation of cortical taste circuits revealed by granger causality with signal-dependent noise. *PLoS Comput Biol*. 9:e1003265.

21 Farb NAS, Segal ZV, Anderson AK. 2013. Attentional modulation of primary interoceptive and exteroceptive cortices. *Cereb Cortex*. 23:114–126.

22 Petzschner FH, *et al.* 2019. Focus of attention modulates the heartbeat evoked potential. *NeuroImage*. 186:595–606.

23 Criscuolo A, Schwartze M, Kotz SA. 2022. Cognition through the lens of a body-brain dynamic system. *Trends Neurosci*. 45:667–677.

24 Shaffer F, McCraty R, Zerr CL. 2014. A healthy heart is not a metronome: an integrative review of the heart's anatomy and heart rate variability. *Front Psychol*. 5:1040.

25 Schandry R, Sparrer B, Weitkunat R. 1986. From the heart to the brain: a study of heartbeat contingent scalp potentials. *Int J Neurosci*. 30:261–275.

26 Coll M-P, Hobson H, Bird G, Murphy J. 2021. Systematic review and meta-analysis of the relationship between the heartbeat-evoked potential and interoception. *Neurosci Biobehav Rev*. 122:190–200.

27 Montoya P, Schandry R, Müller A. 1993. Heartbeat evoked potentials (HEP): topography and influence of cardiac awareness and focus of attention. *Electroencephalogr Clin Neurophysiol*. 88:163–172.

28 Yuan H, Yan HM, Xu XG, Han F, Yan Q. 2007. Effect of heartbeat perception on heartbeat evoked potential waves. *Neurosci Bull*. 23:357–362.

29 Pollatos O, Schandry R. 2004. Accuracy of heartbeat perception is reflected in the amplitude of the heartbeat-evoked brain potential. *Psychophysiology*. 41:476–482.

30 Lechinger J, Heib DPJ, Gruber W, Schabus M, Klimesch W. 2015. Heartbeat-related EEG amplitude and phase modulations from wakefulness to deep sleep: interactions with sleep spindles and slow oscillations. *Psychophysiology*. 52:1441–1450.

31 Calderone DJ, Lakatos P, Butler PD, Castellanos FX. 2014. Entrainment of neural oscillations as a modifiable substrate of attention. *Trends Cogn Sci*. 18:300–309.

32 Clayton MS, Yeung N, Cohen Kadosh R. 2015. The roles of cortical oscillations in sustained attention. *Trends Cogn Sci*. 19:188–195.

33 Henry MJ, Herrmann B. 2014. Low-frequency neural oscillations support dynamic attending in temporal context. *Timing Time Percept*. 2:62–86.

34 Klimesch W. 2012. Alpha-band oscillations, attention, and controlled access to stored information. *Trends Cogn Sci*. 16:606–617.

35 Schroeder CE, Lakatos P. 2009. Low-frequency neuronal oscillations as instruments of sensory selection. *Trends Neurosci*. 32:9–18.

36 Kritzman L, *et al.* 2022. Steady-state visual evoked potentials differentiate between internally and externally directed attention. *NeuroImage*. 254:119133.

37 Villena-González M, *et al.* 2017. Attending to the heart is associated with posterior alpha band increase and a reduction in sensitivity to concurrent visual stimuli. *Psychophysiology*. 54:1483–1497.

38 García-Cordero I, *et al.* 2017. Attention, in and out: scalp-level and intracranial EEG correlates of interoception and exteroception. *Front Neurosci*. 11:411.

39 Agus TR, Thorpe SJ, Pressnitzer D. 2010. Rapid formation of robust auditory memories: insights from noise. *Neuron*. 66:610–618.

40 Agus TR, Pressnitzer D. 2013. The detection of repetitions in noise before and after perceptual learning. *J Acoust Soc Am*. 134:464–473.

41 Andrillon T, Kouider S, Agus T, Pressnitzer D. 2015. Perceptual learning of acoustic noise generates memory-evoked potentials. *Curr Biol*. 25:2823–2829.

42 Luo H, Tian X, Song K, Zhou K, Poeppel D. 2013. Neural response phase tracks how listeners learn new acoustic representations. *Curr Biol*. 23:968–974.

43 Ringer H, Schröger E, Grimm S. 2023. Perceptual learning of random acoustic patterns: impact of temporal regularity and attention. *Eur J Neurosci*. 57:2112–2135.

44 Claassen J, *et al.* 2019. Detection of brain activation in unresponsive patients with acute brain injury. *N Engl J Med*. 380:2497–2505.

45 Cruse D, *et al.* 2011. Bedside detection of awareness in the vegetative state: a cohort study. *Lancet*. 378:2088–2094.

46 Owen AM, *et al.* 2006. Detecting awareness in the vegetative state. *Science*. 313:1402–1402.

47 Giacino JT, Fins JJ, Laureys S, Schiff ND. 2014. Disorders of consciousness after acquired brain injury: the state of the science. *Nat Rev Neurol*. 10:99–114.

48 Fischer DB, Truog RD. 2015. What is a reflex? A guide for understanding disorders of consciousness. *Neurology*. 85:543–548.

49 Giacino JT, *et al.* 2009. Behavioral assessment in patients with disorders of consciousness: gold standard or fool's gold? *Prog Brain Res*. 177:33–48.

50 Schnakers C, *et al.* 2009. Diagnostic accuracy of the vegetative and minimally conscious state: clinical consensus versus standardized neurobehavioral assessment. *BMC Neurol*. 9:35.

51 Schiff ND. 2015. Cognitive motor dissociation following severe brain injuries. *JAMA Neurol*. 72:1413–1415.

52 Laureys S, *et al.* 2005. The locked-in syndrome: what is it like to be conscious but paralyzed and voiceless? *Prog Brain Res*. 150:495–611.

53 Bruno MA, *et al.* 2010. Disorders of consciousness: moving from passive to resting state and active paradigms. *Cogn Neurosci*. 1: 193–203.

54 Lendner JD, *et al.* 2020. An electrophysiological marker of arousal level in humans. *eLife*. 9:e55092.

55 Voytek B, Knight RT. 2015. Dynamic network communication as a unifying neural basis for cognition, development, aging, and disease. *Biol Psychiatry*. 77:1089–1097.

56 Zaccaro A, Perrucci MG, Parrotta E, Costantini M, Ferri F. 2022. Brain-heart interactions are modulated across the respiratory cycle via interoceptive attention. *NeuroImage*. 262:119548.

57 Allen M, Levy A, Parr T, Friston KJ. 2022. In the Body's Eye: the computational anatomy of interoceptive inference. *PLoS Comput Biol*. 18:e1010490.

58 Barrett LF, Simmons WK. 2015. Interoceptive predictions in the brain. *Nat Rev Neurosci*. 16:419–429.

59 Seth AK, Suzuki K, Critchley HD. 2012. An interoceptive predictive coding model of conscious presence. *Front Psychol*. 2:395.

60 Ainley V, Apps MAJ, Fotopoulou A, Tsakiris M. 2016. "Bodily precision": a predictive coding account of individual differences in interoceptive accuracy. *Philos Trans R Soc B Biol Sci*. 371: 20160003.

61 Park HD, *et al.* 2018. Neural sources and underlying mechanisms of neural responses to heartbeats, and their role in bodily self-consciousness: an intracranial EEG study. *Cereb Cortex*. 28: 2351–2364.

62 Kim J, Jeong B. 2019. Heartbeat induces a cortical theta-synchronized network in the resting state. *eNeuro*. 6: ENEURO.0200-19.2019.

63 Körmendi J, Ferentzi E, Köteles F. 2022. A heartbeat away from a valid tracking task. An empirical comparison of the mental and the motor tracking task. *Biol Psychol*. 171:108328.

64 Ring C, Brener J. 1996. Influence of beliefs about heart rate and actual heart rate on heartbeat counting. *Psychophysiology*. 33: 541–546.

65 Khalsa SS, Rudrauf D, Feinstein JS, Tranel D. 2009. The pathways of interoceptive awareness. *Nat Neurosci*. 12:1494–1496.

66 Zaccaro A, *et al.* 2024. Attention to cardiac sensations enhances the heartbeat-evoked potential during exhalation. *iScience*. 27:109586.

67 Linden DEJ. 2005. The P300: where in the brain is it produced and what does it tell us? *Neuroscientist*. 11:563–576.

68 Chun MM, Golomb JD, Turk-Browne NB. 2011. A taxonomy of external and internal attention. *Annu Rev Psychol*. 62:73–101.

69 Baird B, Smallwood J, Lutz A, Schooler JW. 2014. The decoupled mind: mind-wandering disrupts cortical phase-locking to perceptual events. *J Cogn Neurosci*. 26:2596–2607.

70 Barron E, Riby LM, Greer J, Smallwood J. 2011. Absorbed in thought: the effect of mind wandering on the processing of relevant and irrelevant events. *Psychol Sci*. 22:596–601.

71 Kam JWY, *et al.* 2011. Slow fluctuations in attentional control of sensory Cortex. *J Cogn Neurosci*. 23:460–470.

72 Kam JWY, *et al.* 2021. Top–down attentional modulation in human frontal cortex: differential engagement during external and internal attention. *Cereb Cortex*. 31:873–883.

73 Villena-González M, López V, Rodríguez E. 2016. Orienting attention to visual or verbal/auditory imagery differentially impairs the processing of visual stimuli. *NeuroImage*. 132: 71–78.

74 Ceh SM, *et al.* 2020. Neurophysiological indicators of internal attention: an electroencephalography–eye-tracking coregistration study. *Brain Behav*. 10:e01790.

75 Cooper NR, Croft RJ, Dominey SJJ, Burgess AP, Gruzelier JH. 2003. Paradox lost? Exploring the role of alpha oscillations during externally vs. internally directed attention and the implications for idling and inhibition hypotheses. *Int J Psychophysiol*. 47:65–74.

76 Foxe JJ, Snyder AC. 2011. The role of alpha-band brain oscillations as a sensory suppression mechanism during selective attention. *Front Psychol*. 2:154.

77 Kam JWY, Solbakk A-K, Endestad T, Meling TR, Knight RT. 2018. Lateral prefrontal cortex lesion impairs regulation of internally and externally directed attention. *NeuroImage*. 175:91–99.

78 Magosso E, Ricci G, Ursino M. 2021. Alpha and theta mechanisms operating in internal-external attention competition. *J Integr Neurosci*. 20:1–19.

79 Braboszcz C, Delorme A. 2011. Lost in thoughts: neural markers of low alertness during mind wandering. *NeuroImage*. 54:3040–3047.

80 Van Son D, *et al.* 2019. Frontal EEG theta/beta ratio during mind wandering episodes. *Biol Psychol*. 140:19–27.

81 Colombo MA, *et al.* 2019. The spectral exponent of the resting EEG indexes the presence of consciousness during unresponsiveness induced by propofol, xenon, and ketamine. *NeuroImage*. 189:631–644.

82 Gao R, Peterson EJ, Voytek B. 2017. Inferring synaptic excitation/inhibition balance from field potentials. *NeuroImage*. 158:70–78.

83 Pertermann M, Bluschke A, Roessner V, Beste C. 2019. The modulation of neural noise underlies the effectiveness of methylphenidate treatment in attention-deficit/hyperactivity disorder. *Biol Psychiatry Cogn Neurosci Neuroimaging*. 4:743–750.

84 Pertermann M, Mückschel M, Adelhöfer N, Ziemssen T, Beste C. 2019. On the interrelation of $1/f$ neural noise and norepinephrine system activity during motor response inhibition. *J Neurophysiol*. 121:1633–1643.

85 Zhang C, Stock A-K, Mückschel M, Hommel B, Beste C. 2023. Aperiodic neural activity reflects metacontrol. *Cereb Cortex*. 33: 7941–7951.

86 Stam CJ. 2005. Nonlinear dynamical analysis of EEG and MEG: review of an emerging field. *Clin Neurophysiol*. 116:2266–2301.

87 Kam JWY, Rahnuma T, Park YE, Hart CM. 2022. Electrophysiological markers of mind wandering: a systematic review. *NeuroImage*. 258:119372.

88 Missonnier P, *et al.* 2006. Frontal theta event-related synchronization: comparison of directed attention and working memory load effects. *J Neural Transm*. 113:1477–1486.

89 Wascher E, *et al.* 2014. Frontal theta activity reflects distinct aspects of mental fatigue. *Biol Psychol*. 96:57–65.

90 Cavanagh JF, Frank MJ. 2014. Frontal theta as a mechanism for cognitive control. *Trends Cogn Sci*. 18:414–421.

91 Candia-Rivera D, *et al*. 2021. Neural responses to heartbeats detect residual signs of consciousness during resting state in post-comatose patients. *J Neurosci*. 41:5251–5262.

92 Candia-Rivera D, Machado C. 2023. Multidimensional assessment of heartbeat-evoked responses in disorders of consciousness. *Eur J Neurosci*. 58:3098–3110.

93 Raimondo F, *et al*. 2017. Brain–heart interactions reveal consciousness in noncommunicating patients. *Ann Neurol*. 82:578–591.

94 Sitt JD, *et al*. 2014. Large scale screening of neural signatures of consciousness in patients in a vegetative or minimally conscious state. *Brain*. 137:2258–2270.

95 Peirce JW. 2007. PsychoPy-Psychophysics software in python. *J Neurosci Methods*. 162:8–13.

96 Gramfort A, *et al*. 2013. MEG and EEG data analysis with MNE-python. *Front Neurosci*. 7:267.

97 Jas M, Engemann DA, Bekhti Y, Raimondo F, Gramfort A. 2017. Autoreject: automated artifact rejection for MEG and EEG data. *NeuroImage*. 159:417–429.

98 Dirlich G, Vogl L, Plaschke M, Strian F. 1997. Cardiac field effects on the EEG. *Electroencephalogr Clin Neurophysiol*. 102: 307–315.

99 Freund Y, Schapire RE. 1997. A decision-theoretic generalization of on-line learning and an application to boosting. *J Comput Syst Sci*. 55:119–139.

100 Pedregosa F, *et al*. 2011. Scikit-learn: machine learning in {P}ython. *J Mach Learn Res*. 12:2825–2830.

101 Combrisson E, Jerbi K. 2015. Exceeding chance level by chance: the caveat of theoretical chance levels in brain signal classification and statistical assessment of decoding accuracy. *J Neurosci Methods*. 250:126–136.

102 Benjamini Y, Hochberg Y. 1995. Controlling the false discovery rate: a practical and powerful approach to multiple testing. *J R Stat Soc Ser B Methodol*. 57:289–300.

103 Kayser J, Tenke CE. 2015. On the benefits of using surface Laplacian (current source density) methodology in electrophysiology. *Int J Psychophysiol*. 97:171–173.

104 Engemann DA, *et al*. 2018. Robust EEG-based cross-site and cross-protocol classification of states of consciousness. *Brain*. 141:3179–3192.

105 Willacker L, *et al*. 2022. PerBrain: a multimodal approach to personalized tracking of evolving state-of-consciousness in brain-injured patients: protocol of an international, multicentric, observational study. *BMC Neurol*. 22:468.

106 Giacino JT, Kalmar K, Whyte J. 2004. The JFK coma recovery scale-revised: measurement characteristics and diagnostic utility. *Arch Phys Med Rehabil*. 85:2020–2029.

107 Bekinschtein TA, *et al*. 2009. Neural signature of the conscious processing of auditory regularities. *Proc Natl Acad Sci U S A*. 106:1672–1677.